Lanthanum anomalies as fingerprints of methanotrophy

X. Wang, Jean-Alix J-A Barrat, G. Bayon, Laurent Chauvaud, D. L Feng

Geochemical Perspectives Letters

Lanthanum anomalies as fingerprints of methanotrophy

X. Wang[1,4], J.-A. Barrat[2,3*], G. Bayon[4], L. Chauvaud[3], D. Feng[1]

OPEN ACCESS

doi: 10.7185/geochemlet.2019

Abstract

Methane is an important greenhouse gas whose emissions into the oceans and atmosphere are regulated by relatively unconstrained anaerobic and aerobic microbial processes. The aerobic pathway for methane oxidation is thought to be largely dependent upon the use of rare earth elements (REE), but to date the effects of this process on their abundances in bacteria or in organisms living in symbiosis with methanotrophs remain to be evaluated. Here we show that deep sea chemosynthetic mussels prospering at methane seeps display distinctive lanthanum enrichments linked to the enzymatic activities of their symbionts. These results demonstrate that methanotrophy is able to fractionate efficiently REE distributions in organisms and possibly in the environment. Lanthanum anomalies recorded in ancient sediments are potential chemical fossils that could be used in the geological record for tracking early evidence of microbial life.

Received 9 March 2020 | Accepted 18 May 2020 | Published 2 July 2020

Introduction

Until recently, REEs were assumed to have no manifest biological function. The discovery of a REE dependent enzyme involved in the metabolism of aerobic methanotrophic bacteria has radically changed this view (Pol *et al.*, 2014; Semrau *et al.*, 2018; Cotruvo, 2019), showing that these elements could be essential for microbial life. Methanotrophic bacteria first convert methane to methanol. This first step of aerobic methane oxidation is followed by the degradation of methanol into formaldehyde using methanol dehydrogenase enzymes. These enzymes are either Ca dependent (MxaF type) or light REE dependent (XoxF type) (Skovran *et al.*, 2011). However, the latter XoxF type seems to be more frequently used by marine bacteria (Ramachandran *et al.*, 2015; Taubert *et al.*, 2015), hence suggesting that REEs could play a previously unsuspected and important role in the development of marine ecosystems relying on aerobic methanotrophic symbioses.

At ocean margins, areas of active methane seepage at the seafloor (or cold seeps) typically host abundant macrofaunal communities, which derive the vast majority of their nutrition from symbiotic chemotrophic microbes hosted in their gills. The dominant biogeochemical reaction at cold seeps is the anaerobic oxidation of methane (AOM) typically coupled with sulphate reduction, a process that is mediated by a consortium of anaerobic methanotrophic archaea and sulphate reducing bacteria (Boetius *et al.*, 2000). While a substantial fraction of the macrofauna at methane seeps relies on anaerobic microbial symbionts (mostly using dissolved sulphide, such as tubeworms and clams), mussels are instead commonly associated with aerobic methanotrophic symbionts. In this study, we analysed a series of well characterised shellfish samples from two active seepage sites (Haima and Site F) located in the South China Sea (Feng *et al.*, 2015, 2018; Liang *et al.*, 2017). Our sampling includes both methanotrophic (*Gigantidas platifrons* and *Gigantidas haimaensis*) and thiotrophic mussels (*Bathymodiolus aduloides*), in addition to other bivalves (clams) associated with sulphur oxidising bacteria (*Calyptogena marissinica*). For comparison, additional thiotrophic clams from the Nankai Trough (Fiala-Médioni *et al.*, 1993), and a series of heterotrophic blue mussels (*Mytilus edulis*) devoid of any chemotrophic symbionts from coastal waters of France were also analysed (Table S-1). Methods are described in Supplementary Information.

Results and Discussion

The abundances of REEs in shellfish samples are low, but highly variable, in both shells and soft tissues (Figs. 1, 2; Tables S-2–8). Most samples display positive yttrium and negative cerium anomalies respectively, which represent conspicuous features of seawater and marine-derived materials such as biogenic carbonates. A striking feature of our results is that methanotrophic mussels display shale normalised distribution patterns that strongly differ from the other studied shellfish samples. Compared to the thiotrophic shellfish samples, the shells and soft tissues (feet, mantles) of methanotrophic mussels are

1. Shanghai Engineering Research Center of Hadal Science and Technology, College of Marine Sciences, Shanghai Ocean University, Shanghai 201306, China
2. Université de Bretagne Occidentale, Brest, CNRS, UMR 6538 (Laboratoire Géosciences Océan), Institut Universitaire Européen de la Mer (IUEM), Place Nicolas Copernic, 29280 Plouzané, France
3. Université de Bretagne Occidentale, Brest, CNRS, UMR 6539 (Laboratoire des Sciences de l'Environnement Marin), LIA BeBEST, Institut Universitaire Européen de la Mer (IUEM), Place Nicolas Copernic, 29280 Plouzané, France
4. IFREMER, Marine Geosciences Unit, F-29280 Plouzané, France
* Corresponding author (email: barrat@univ-brest.fr)

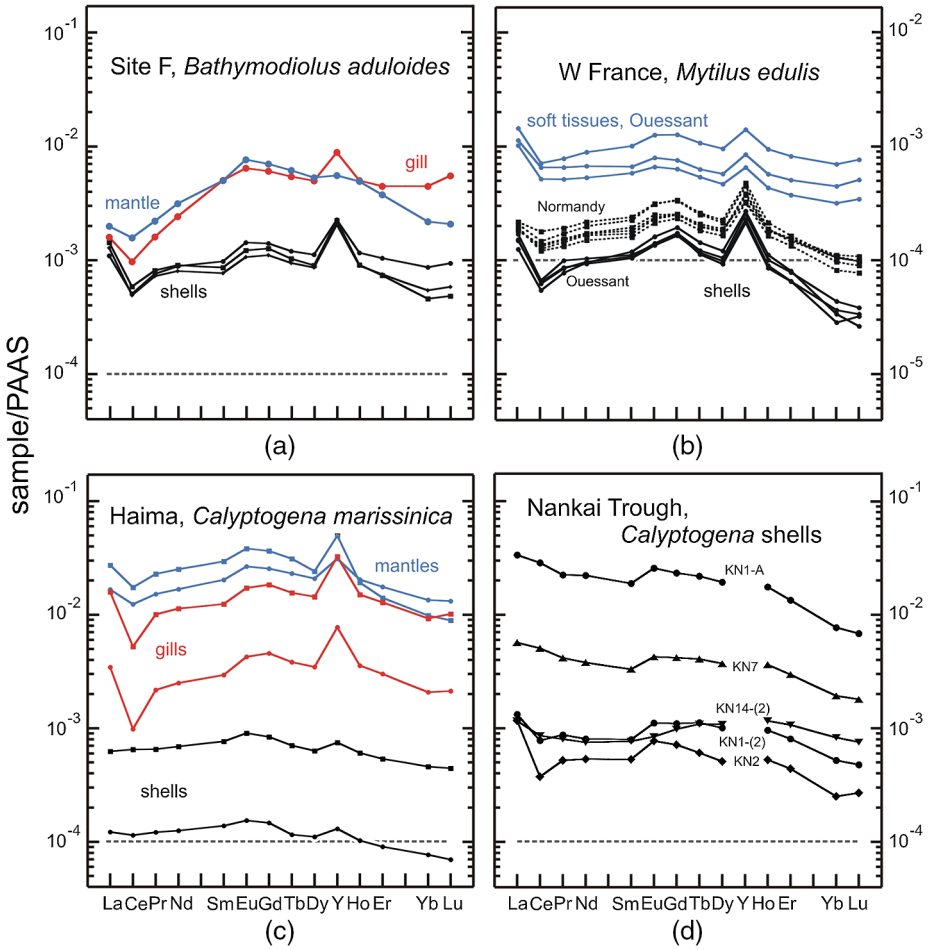

Figure 1 REE + Y patterns normalised to Post Archean Australian Shale (PAAS; Pourmand *et al.*, 2012) for thiotrophic shellfish from cold seeps and for heterotrophic *Mytilus edulis* from France. The grey dashed line corresponds to the 10^{-4} x PAAS level. Notice that the *Bathymodiolus* shells are ten times more REE richer than the *Mytilus* ones.

characterised by often large positive lanthanum anomalies (La/La* = 2.0–5.9; Figs. 2–4, see Supplementary Information for the calculations of the anomalies). Furthermore, their gills exhibit spectacular enrichment in light REEs (Figs. 2, 4).

To a large extent, the shale normalised distribution patterns of REEs in the studied shellfish samples are controlled by variable source contributions to the different organs or tissues. In the case of heterotrophic shellfish from coastal areas, the REEs contained in the soft tissues are mainly derived from suspended particles with a reduced contribution from seawater (Akagi and Edanami, 2017). Shells result from the activity of the mantle epithelium inside specific internal liquid (Wheeler, 1992). Consequently, their REE distribution patterns directly reflect the composition of the mantle, with additional potential inputs from the fluids associated with carbonate secretion. In any case, the corresponding REE patterns differ significantly from typical seawater signatures, more closely resembling those of the soft tissues, dominated by inputs from filtered suspended particles.

Overall, heterotrophic (Bau *et al.*, 2010; Ponnurangam *et al.*, 2016; Akagi and Edanami, 2017; Le Goff *et al.*, 2019) and thiotrophic shellfish both display comparable REE features. The shells of thiotrophic mussels *Bathymodiolus aduloides* and of coastal mussels *Mytilus edulis* (Bau *et al.*, 2010; Ponnurangam *et al.*, 2016 and this work, Table S-7) exhibit very similar REE patterns, albeit being characterised by different REE abundances (Fig. 1). Gill and mantle samples also display similar patterns, both characterised by light REE depletions [$(La/Sm)_{sn}$ = 0.32–0.40] and moderately positive La anomalies (La/La* = 1.83–2.26). In agreement with previous studies (Akagi and Edanami, 2017), soft tissues are enriched in REEs compared to shells. Like previous mussels, the REE patterns of thiotrophic *Calyptogena* display mixed features between those of terrigenous sediments and seawater. Importantly, all these samples plot within the range of La/La* values for seawater (Fig. 3). The same conclusion also applies to the dominantly thiotrophic shellfish collected at hydrothermal fields along oceanic ridges (Bau *et al.*, 2010). Their shells exhibit patterns largely influenced by the composition of hydrothermal fluids but never show any particular lanthanum excesses, suggesting that these animals and their symbionts do not require light REEs (Fig. 3).

The situation for methanotrophic shellfish is clearly different (Figs. 3, 4). Their gills show exceptional enrichments in light REEs, which, to the best of our knowledge, have never been reported for any natural sediments, seafloor rocks or authigenic phases. Other soft tissues and shells also exhibit significant lanthanum enrichments, as well as marked lanthanum anomalies, with La/La* ratios (up to 5) that largely exceed the highest values measured in South China Sea water (La/La* = 2.5; Alibo and Nozaki, 2000). To date, the exchange and recycling of REEs between the different organs of the studied molluscs has never been investigated. However, the exceptional La anomalies reported here cannot be explained by the contribution from any hypothetical fluid or sediment sources. If this was the case,

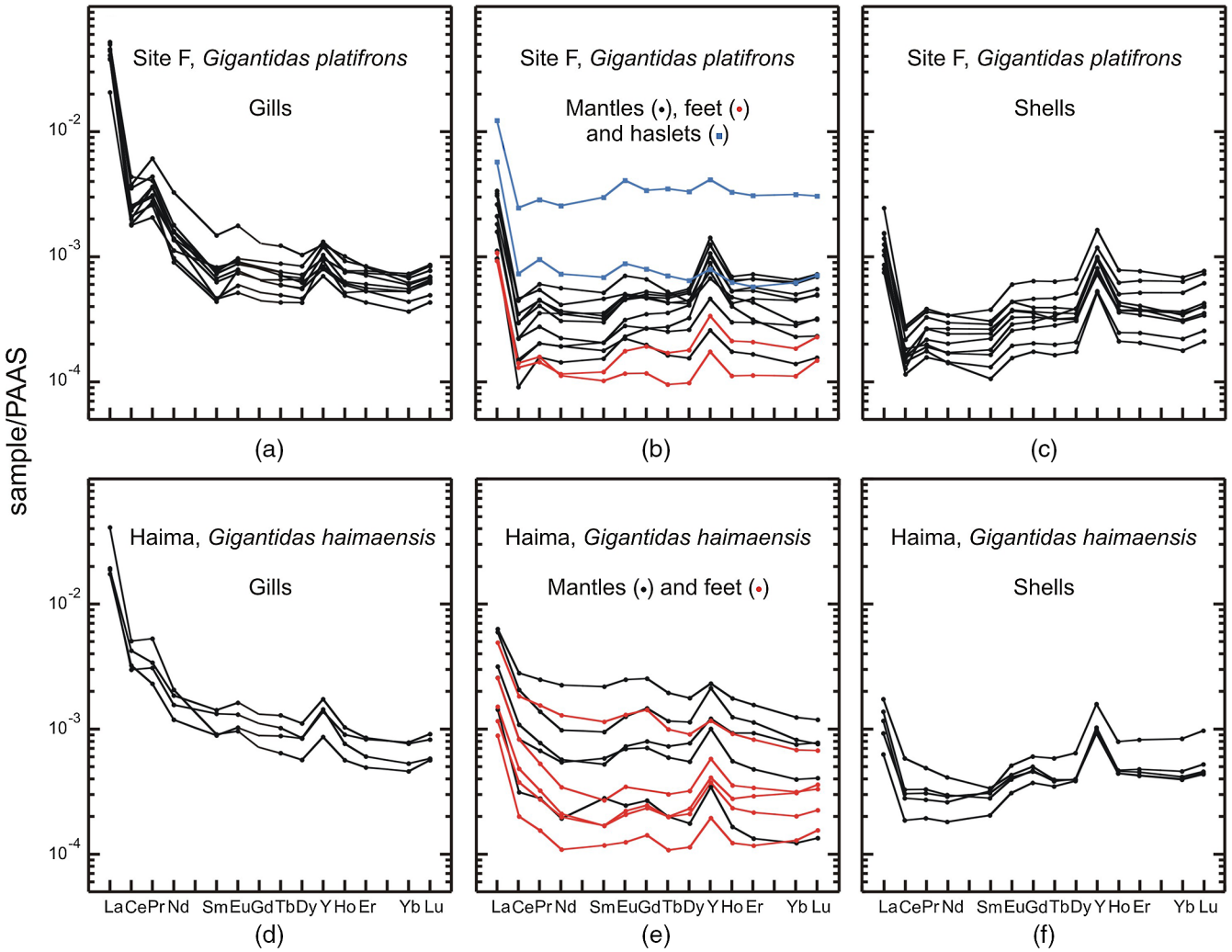

Figure 2 REE + Y patterns normalised to PAAS (Pourmand *et al.*, 2012) for methanotrophic mussels from South China Sea cold seeps.

thiotrophic clams and mussels sampled from the same sites would have also displayed similar La enrichments. Therefore, the specific REE features observed in the methanotrophic shellfish samples are best explained by biological processes. It is very important to note that the gills show the highest enrichments in light REEs and lanthanum abundances, because this is precisely where the methanotrophic symbionts are hosted in these mussels (Barry *et al.*, 2002; Yu *et al.*, 2019). Therefore, the enzymatic activity of the methanotrophic symbionts is the most plausible cause for the selective accumulation of light REEs in the *Gigantidas* gills, and the large lanthanum anomalies in the other soft tissues and recorded in the shells.

An immediate question concerns the presumed source of the light REEs hosted in the mussel gills. Marine sediments are significantly enriched in REEs and contain about 10 million times more lanthanum than seawater, and as such could possibly contribute to the observed light REEs enrichment of the gills, *via* possibly an unrecognised process of remineralisation by the gill cells or by the symbionts. However, it is more likely that most of the light REEs contained in the gills are derived from the fluids filtered by the shellfish. Considering an average mass for *Gigantidas* gill of ~0.7 g (on a dry basis), we can estimate that it contains about 1.9 μg/g lanthanum at Site F, and 1 μg/g at Haima. This corresponds to the quantity of lanthanum contained in about 275 litres of seawater at Site F (or 14.4 litres of pore waters; Himmler *et al.* 2013) and 145 litres of sea water at Haima (or 7.6 litres of pore waters). Whatever the exact composition of the involved fluids, these volumes are very small compared to the volume of water that a mussel can filter every day: ~180 litres, estimated assuming a mussel with 3 g of soft tissues on a dry basis and a rate similar to that of *Mytilus edulis* (Blayne *et al.*, 1989). Based on these considerations, it is very likely that the methanotrophic symbionts hosted in gills can access the light REEs they need from the seawater filtered by the shellfish, without invoking more complex uptake processes. This raises the question as to whether methanotrophic activity at cold seeps could have an impact on the oceanic REE budget, at least in the water column surrounding the seepage sites. We can estimate that about 72 m^3 of water is filtered every day by one square metre of a typical mussel bed with 400 animals. And if we limit our estimate to the amount of lanthanum contained only by gills, the same square metre at Site F contains as much lanthanum as 110 m^3 of seawater. At present, we do not know what proportion of dissolved REEs in the fluids filtered by molluscs are actually taken up by the symbionts, nor what proportions of these are transferred to the organs of the shellfish. However, the biological activity (including not only the mussels that dominate the biomass, but all the other methanotrophs that use XoxF-type enzymes) must necessarily have an impact on the chemistry of seawater near cold seeps. The capability of methanotrophic bacteria to affect the local distribution of REEs in seawater has already been observed in the Gulf of Mexico. Following the

Deepwater Horizon well blowout in 2010, the release of massive methane plumes in the water column was accompanied by substantial removal of light REEs, interpreted as the result of intense methanotrophic activity (Shiller *et al.*, 2017).

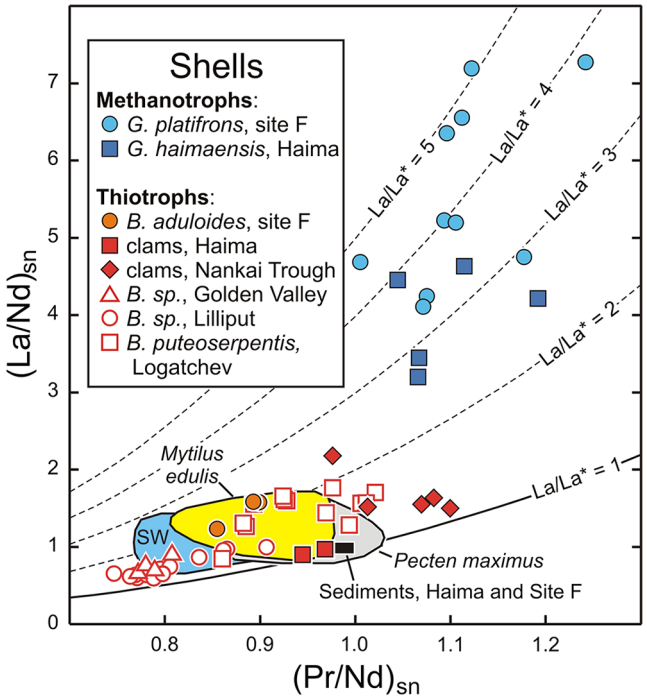

Figure 3 $(La/Nd)_{sn}$ *vs.* $(Pr/Nd)_{sn}$ plot for the shells from various shellfish from cold seeps (this work), from Atlantic hydrothermal sites (Golden Valley, Lilliput and Logatchev; Bau *et al.*, 2010), heterotrophic shellfish (*Mytilus edulis* and *Pecten maximus*; Bau *et al.*, 2010; Ponnurangam *et al.*, 2016; Le Goff *et al.*, 2019 and this work). Fields for seawater (SW; Alibo and Nozaki, 2000) and sediments from Haima and Site F (this work) are shown for comparison.

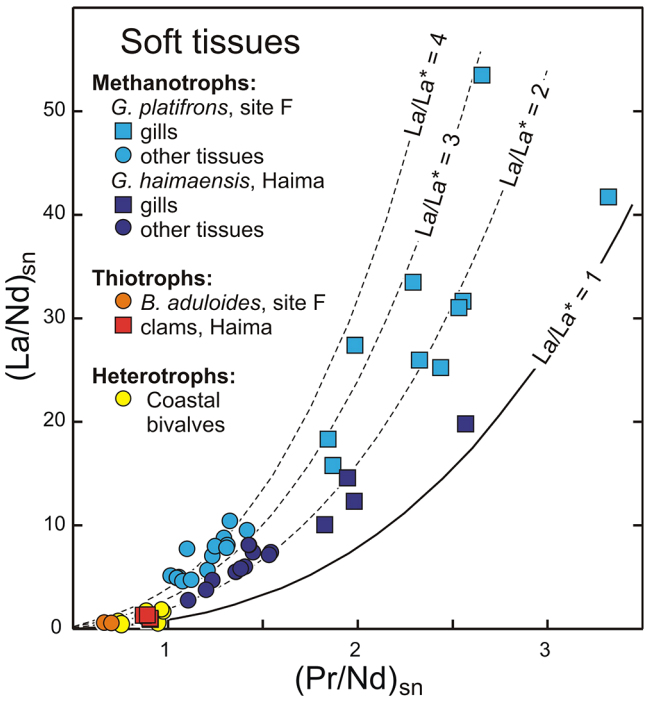

Figure 4 $(La/Nd)_{sn}$ *vs.* $(Pr/Nd)_{sn}$ plot for the soft tissues prepared from various shellfish from cold seeps, and various heterotrophic coastal bivalves (Akagi and Edanami, 2016 and this work).

Our findings could have implications for the understanding of other lanthanum excesses previously identified in seawater and various marine precipitates, but remaining unexplained so far. However, this element was assumed to be more stable than other light REEs during complexation in seawater (de Baar *et al.*, 1985) or could be released from suspended barite particles (Grenier *et al.*, 2018). In marine precipitates, lanthanum anomalies are common features that are usually inferred to be largely inherited from seawater (*e.g.*, Bau and Dulski, 1996; Kamber and Webb, 2001), but for which no clear explanation has been proposed. Our data demonstrate unambiguously that positive lanthanum anomalies can be generated by the enzymatic activity of methanotrophs, hence providing the possibility of promising applications in various fields of research. Importantly, in future studies, the presence of marked lanthanum anomalies or any other large light REE enrichments in fossil shells could be used as proxies for past methanotrophic activity. Methanotrophic organisms have been present since the Archean, but their detection in the geological record, and in the sedimentary archives of the early Earth oceans are still the subject of intense debate (Thomazo *et al.*, 2009; Knoll *et al.*, 2016). In particular, lanthanum anomalies are frequent in ancient microbial carbonates and banded iron formations (Bau and Dulski, 1996; Kamber and Webb, 2001; Planavsky *et al.*, 2010), which may point towards a putative REE dependent microbiological origin. Revisiting the REE geochemistry of these ancient rocks could provide fresh insights into the emergence and diversification of life.

Acknowledgements

We thank Karim Benzerara for the editorial handling, and the anonymous reviewers for constructive comments. ICP-MS analyses were obtained with the help of Bleuenn Gueguen. We are grateful to Jacques Boulègue who provided us the samples from Nankai Trough, Samuel Le Goff for the mussels from Ouessant, Richard Greenwood (Open University) and Michel Rafini (UBO) for discussions and grammatical corrections. We express our sincere appreciation to the crews of the manned submersible *Jiaolong*, ROV *Haima*, ROV *ROPOS*, and the research vessels. This work was supported by the "Laboratoire d'Excellence" LabexMER (ANR-10-LABX-19) and co-funded by grants from the French Government under the programme "Investissements d'Avenir", by the National Program on Global Change and Air-Sea Interaction (GASI-GEOGE-05-04), the National Key R&D Program of China (2017YFC0306702) and the NSF of China (Grants: 41773091, 41730528, and 41761134084). XW acknowledges the China Scholarship Council for supporting a research visit to IFREMER.

Editor: Karim Benzerara

Additional Information

Supplementary Information accompanies this letter at http://www.geochemicalperspectivesletters.org/article2019.

author. Additional information is available at http://www.geochemicalperspectivesletters.org/copyright-and-permissions.

Cite this letter as: Wang, X., Barrat, J.-A., Bayon, G., Chauvaud, L., Feng, D. (2020) Lanthanum anomalies as fingerprints of methanotrophy. *Geochem. Persp. Let.* 14, 26–30.

References

Akagi, T., Edanami, K. (2017) Sources of rare earth elements in shells and soft-tissues of bivalves from Tokyo Bay. *Marine Chemistry* 194, 55–62.

Alibo, D.S., Nozaki, Y. (2000) Dissolved rare earth elements in the South China Sea: geochemical characterization of the water masses. *Journal of Geophysical Research* 105, C12, 28771–28783.

de Baar, H.J.W., Bacon, M.P., Brewer, P.G., Bruland, K.W. (1985) Rare earth elements in the Pacific and Atlantic Oceans. *Geochimica et Cosmochimica Acta* 49, 1943–1959.

Barry, J.P., Buck, K.R., Kochevar, R.K., Nelson, D.C., Fujiwara, Y., Goffredi, S.K., Hashimoto, J. (2002) Methane-based symbiosis in a mussel, Bathymodiolus platifrons, from cold seeps in Sagami Bay, Japan. *Invertebrate Biology* 121, 47–54.

Bau, M., Dulski, P. (1996) Distribution of yttrium and rare-earth elements in the Penge and Kuruman iron-formations, Transvaal Supergroup, South Africa. *Precambrian Research* 79, 37–55.

Bau, M., Balan, S., Schmidt, K., Koschinsky, A. (2010) Rare earth elements in mussel shells of the Mytilidae family as tracers for hidden and fossil high-temperature hydrothermal systems. *Earth and Planetary Science Letters* 299, 310–316.

Blayne, B.L., Hawkins, A.J.S., Navarro, E., Iglesias, I.P. (1989) Effects of seston concentration on feeding, digestion and growth in the mussel *Mytilus edulis*. *Marine Ecology Progress Series* 55, 47–54.

Boetius, A., Ravenschlag, K., Schubert, C.J., Rickert, D., Widdel, F., Gieseke, A., Amann, R., Barker Jørgensen, B., Witte, U., Pfannkuche, O. (2000) A marine microbial consortium apparently mediating anaerobic oxidation of methane. *Nature* 407, 623–626.

Cotruvo, Jr., J.A. (2019) The chemistry of lanthanides in biology: recent discoveries, emerging principles, and technological applications. *ACS Central Science* 5, 1496–1506.

Feng, D., Cheng, M., Kiel, S., Qiu, J.W., Yang, Q., Zhou, H., Peng, Y., Chen, D. (2015) Using *Bathymodiolus* tissue stable carbon, nitrogen and sulfur isotopes to infer biogeochemical process at a cold seep in the South China Sea. *Deep-Sea Research I* 104, 52–59.

Feng, D., Peckmann, J., Li, N., Kiel, S., Qiu, J.W., Liang, Q., Carney, R.S., Peng, Y., Tao, J., Chen, D. (2018) The stable isotope fingerprint of chemosymbiosis in the shell organic matrix of seep-dwelling bivalves. *Chemical Geology* 479, 241–250.

Fiala-Médioni, A., Boulègue, J., Ohta, S., Felbeck, H., Mariotti, A. (1993) Source of energy sustaining the *Calyptogena* populations from deep trenches in subduction zones off Japan. *Deep-Sea Research 1,* 40, 6,1241–1258.

Grenier, M, Garcia-Solsona, E., Lemaitre, N., Trull, T.W., Bouvier, V., Nonnotte, P., van Beek, P., Souhaut, M., Lacan, F., Jeandel, C. (2018) Differentiating lithogenic supplies, water mass transport, and biological processes on and off the Kerguelen Plateau using rare earth element concentrations and neodymium isotopic compositions. *Frontiers in Marine Science* 5, 426.

Himmler, T., Haley, B.A., Torres, M.E., Klinkhammer, G.P., Bohrmann, G., Peckmann, J. (2013) Rare earth element geochemistry in cold-seep pore waters of Hydrate Ridge, northeast Pacific Ocean. *Geo-Marine Letters* 33, 369–379.

Kamber, B.S., Webb, G.E. (2001) The geochemistry of late Archaean microbial carbonate: Implications for ocean chemistry and continental erosion history. *Geochimica et Cosmochimica Acta* 65, 2509–2525.

Knoll, A.H., Bergmann, K.D., Strauss, J.V. (2016) Life: the first two billion years. *Philosophical Transactions of the Royal Society B* B371, 20150493.

Le Goff, S, Barrat, J.A., Chauvaud, L., Paulet, Y.M., Gueguen, B., Ben Salem, D. (2019) Compound-specific recording of gadolinium pollution in coastal waters by great scallops. *Scientific Reports* 9, 8015.

Liang, Q., Hu, Y., Feng, D., Peckmann, J., Chen, L., Yang, S., Liang, J., Tao, J., Chen, D. (2017) Authigenic carbonates from two newly discovered active cold seeps on the northwestern slope of the South China Sea: Constraints on fluids sources, formation environments and seepage dynamics. *Deep Sea Research I* 124, 31–41.

Planavsky, N., Bekker, A., Rouxel, O.J., Kamber, B., Hofmann, A., Knudsen A., Lyons, T.W. (2010) Rare Earth Element and yttrium compositions of Archean and Paleoproterozoic Fe formations revisited: new perspectives on the significance and mechanisms of deposition. *Geochimica et Cosmochimica Acta* 74, 6387–6405.

Pol, A., Barends, T.R.M., Dietl, A., Khadem, A.F., Eygensteyn, J., Jetten, M.S.M., Op den Camp, H.J.M. (2014) Rare earth metals are essential for methanotrophic life in volcanic mudpots. *Environmental Microbiology* 16, 255–264.

Ponnurangam, A., Bau, M., Brenner, M., Kochinsky, A. (2016) Mussel shells of Mytilus edulis as bioarchives of the distribution of rare earth elements and yttrium in seawater and the potential impact of pH and temperature on their partitioning behavior. *Biogeosciences* 13, 751–760.

Pourmand, A., Dauphas, N., Ireland, T.J. (2012) A novel extraction chromatography and MC-ICP-MS technique for rapid analysis of REE, Sc and Y: Revising CI-chondrite and Post-Archean Australian Shale (PAAS) abundances. *Chemical Geology* 291, 38–54.

Ramachandran, A., Walsh, D.A. (2015) Investigation of XoxF methanol dehydrogenases reveals new methylotrophic bacteria in pelagic marine and freshwater ecosystems. *FEMS Microbiology Ecology* 91, fiv105.

Semrau, J.D., DiSpirito, A.A., Gu, W., Yoon, S. (2018) Metals and Methanotrophy. *Applied and Environmental Microbiology* 84, e02289–17.

Shiller, A.M., Chan, E.W., Joung D.J., Redmond, M.C., Kessler, J.D. (2017) Light rare earth element depletion during *Deepwater Horizon* blowout methanotrophy. *Scientific Reports* 7, 10389, doi:10.1038/s41598-017-11060-z.

Skovran, E., Palmer, A.D., Rountree, A.M., Good, N.M., Lidstrom, M.E. (2011) XoxF is required for expression of methanol dehydrogenase in Methylobacterium extorquens AM1. *Journal of Bacteriology* 193, 6032–6038.

Taubert, M., Grob, C., Howat, A.M., Burns, O.J., Dixon, J.L., Chen, Y., Colin Murrell, J. (2015) XoxF encoding an alternative methanol dehydrogenase is widespread in coastal marine environments. *Environmental Microbiology* 17, 3937–3948.

Thomazo C., Ader M., Farquhar J., Philippot P. (2009) Methanotrophs regulated atmospheric sulfur isotope anomalies during the MesoArchaean (Tumbiana Formation, Western Australia). *Earth and Planetary Science Letters* 279, 65–75.

Wheeler, A.P. (1992) Mechanisms of molluscan shell formation. In: Bonucci, E. (Ed.) *Calcification in biological systems*. CRC press, Boca Raton, FL, 179–226.

Yu, J., Wang, M., Liu, B., Yue, X., Li, C. (2019) Gill symbionts of the cold-seep mussel Bathymodiolus platifrons: Composition, environmental dependency and immune control. *Fish and Shellfish Immunology* 86, 246–252.

Geochemical Perspectives Letters

Lanthanum anomalies as fingerprints of methanotrophy

X. Wang, J.A. Barrat, G. Bayon, L. Chauvaud, D. Feng

Supplementary Information

The Supplementary Information includes:

- Methods
- Tables S-1 to S-9

Methods

Once on board the ship, the bivalves were sampled by dissecting pieces of soft tissues and shell from the same organism. The soft tissues were rinsed with deionised water to remove residual seawater, and freeze dried. Shells were scrapped to remove traces of soft tissues and sediments, rinsed with deionised water and dried. For each sample, about 100 mg were spiked with a solution of pure Tm and digested in a Teflon beaker by HNO_3 (carbonate), sequentially by HNO_3/H_2O_2 and HNO_3 (soft tissue), or by HF/HNO_3, HNO_3 and HCl (sediments). REEs have been separated from the major elements and concentrated before analysis (Barrat *et al.*, 1996, 2020). Abundances in most samples were determined using a high-resolution inductively coupled plasma-mass spectrometer Thermo Element XR at Institut Universitaire Européen de la Mer (IUEM), Plouzané, France. Each sample was analysed in duplicate or in triplicate, and the results were averaged (Barrat *et al.*, 2016). Results on a carbonate standard obtained during the sessions are given in Table S-9. Clam shells from Nankai Trough were analysed using a similar procedure at Laboratoire de Géodynamique des Chaines Alpines (Université Joseph Fourier, Grenoble) using a Fisons PQ2+ instrument.

The La and Ce anomalies are calculated using the La/La* and Ce/Ce* ratios, where La* and Ce* are the extrapolated La and Ce concentration for a smooth Post Archean Australian Shale-normalised REE pattern and X_{sn} is the concentration of element X normalised to PAAS: $La_{sn}^* = Pr_{sn}^3/Nd_{sn}^2$ and $Ce_{sn}^* = Pr_{sn}^2/Nd_{sn}$. Based on standards and sample replicates, the precisions for abundances and element ratios are usually much better than 5 % (2 RSD).

Table S-1 Samples and location of the sampling localities.

Site	latitude longitude	Cruise	Sampling date	Depth	Sample ID	Species	Chemotrophic symbionts
Nankai Trough	33.66°N 137.90°E	Kaiko-Nankai Nautile manned submersible	08-08-1989 to 09-10-1989	3848 m	KN1-(2), KN1-(A)	*Calyptogena sp.*	Thiotrophs
				2170 m	KN2	*Calyptogena sp.*	Thiotrophs
				3787 m	KN7	*Calyptogena sp.*	Thiotrophs
				2200 m	KN14-(2)	*Calyptogena sp.*	Thiotrophs
Site F	22.12°N 119.29°E	*Jiaolong* manned submersible *ROPOS* ROV	6-18-2013 5-13-2018	1120 m	BA1 to 3	*Bathylomodius aduloides*	Thiotrophs
				1120 m	GP1 to 10	*Gigantidas platifrons*	Methanotrophs
Haima	16.73°N 110.48°E	*Haima* ROV	5-30-2018	1390 m	GH1 to 5	*Gigantidas haimaensis*	Methanotrophs
			5-30-2018	1390 m	CM1 to 2	*Calyptogena marissinica*	Thiotrophs
Ouessant	48.4522°N 5.0971°W		feb-18	0	Ou1 to 4	*Mytilus edulis*	none
Chausey	48.8886°N 1.7863°W		nov-19	0	Ch1 to 3	*Mytilus edulis*	none
Gouville/Mer	49.0916°N 1.6197°W		nov-19	0	Go1 to 3	*Mytilus edulis*	none

Table S-2 REE and Y abundances (in ng/g) in *Gigantidas platifrons* from site F (S : shell ; F: foot; G : gill ; H: haslet; M : mantle; n.a.: not analysed).

	Y	La	Ce	Pr	Nd	Sm	Eu	Gd	Tb	Dy	Ho	Er	Yb	Lu	Ce/Ce*	La/La*
Shells																
GP1, S	25.8	68.3	14.4	2.68	9.00	1.67	0.46	2.19	0.32	1.87	0.43	1.17	0.94	0.16	0.56	4.83
GP2, S	22.1	55.7	11.2	2.72	9.95	1.81	0.45	2.14	0.28	1.69	0.38	1.06	0.91	0.15	0.47	4.62
GP3, S	26.5	109	24.6	3.88	12.71	2.11	0.53	2.37	0.35	2.03	0.45	1.24	1.03	0.18	0.65	5.09
GP4, S	19.6	38.3	14.0	2.21	7.55	1.52	0.40	2.00	0.28	1.73	0.39	1.14	1.06	0.17	0.68	3.42
GP5, S	27.2	49.9	13.8	1.92	6.37	1.24	0.35	1.82	0.30	2.06	0.53	1.59	1.55	0.27	0.74	4.77
GP6, S	20.8	35.7	16.2	2.01	6.29	1.13	0.31	1.63	0.25	1.63	0.39	1.16	1.10	0.19	0.78	2.92
GP7, S	44.8	62.3	23.3	3.69	12.68	2.60	0.73	3.87	0.57	3.54	0.82	2.36	2.06	0.34	0.68	3.35
GP8, S	14.5	33.4	10.1	1.59	5.36	0.91	0.24	1.23	0.18	1.11	0.26	0.76	0.66	0.11	0.67	4.00
GP9, S	14.1	45.9	12.7	1.78	5.28	0.73	0.19	1.05	0.15	0.93	0.22	0.63	0.54	0.09	0.66	3.80
GP10, S	32.3	68.8	19.2	3.33	11.08	1.99	0.53	2.79	0.42	2.72	0.65	1.97	1.91	0.32	0.60	3.85
Gills																
GP1, G	19.2	2322	185	26.2	36.3	3.22	0.71	n.a.	0.44	2.47	0.52	1.33	1.10	0.19	0.31	2.87
GP2, G	34.0	1817	208	37.0	58.5	4.61	0.96	n.a.	0.58	3.49	0.79	2.28	2.12	0.37	0.28	2.07
GP3, G	32.8	1709	161	28.1	52.2	5.42	1.13	n.a.	0.63	3.59	0.81	2.37	2.20	0.38	0.33	3.53
GP4, G	25.4	1974	177	36.2	52.2	3.16	0.63	n.a.	0.38	2.29	0.54	1.63	1.58	0.28	0.22	1.91
GP5, G	28.2	2027	226	31.5	50.6	4.33	0.90	n.a.	0.53	2.99	0.66	1.86	1.67	0.29	0.36	2.80
GP6, G	36.1	2225	384	41.2	59.9	5.21	1.18	n.a.	0.79	4.49	0.97	2.58	2.03	0.34	0.42	1.92
GP7, G	26.4	2025	311	44.4	67.1	5.04	1.06	n.a.	0.68	3.81	0.81	2.18	1.79	0.30	0.33	1.75
GP8, G	21.7	1680	218	30.4	33.7	3.02	0.95	n.a.	0.53	2.95	0.63	1.64	1.32	0.22	0.25	1.14
GP9, G	34.0	2312	329	62.1	122	10.2	2.15	n.a.	1.10	5.49	1.06	2.55	1.85	0.30	0.33	2.44
GP10, G	22.8	917	158	20.9	41.8	5.69	1.10	n.a.	0.64	3.31	0.65	1.72	1.59	0.27	0.47	2.94

Table S-2 (continued) REE and Y abundances (in ng/g) in *Gigantidas platifrons* from site F (S : shell ; F: foot; G : gill ; H: haslet; M : mantle).

	Y	La	Ce	Pr	Nd	Sm	Eu	Gd	Tb	Dy	Ho	Er	Yb	Lu	Ce/Ce*	La/La*
Mantles																
GP1, M	24.4	49.7	8.02	1.60	5.35	1.05	0.28	1.61	0.24	1.72	0.45	1.42	1.34	0.22	0.53	5.86
GP2, M	33.7	143	26.4	4.12	11.4	2.07	0.56	3.03	0.43	2.82	0.69	2.04	1.84	0.30	0.56	4.51
GP3, M	27.5	81.2	19.7	3.60	13.1	2.44	0.59	2.82	0.38	2.36	0.56	1.65	1.37	0.22	0.62	5.01
GP4, M	34.1	137	26.1	4.59	13.0	2.19	0.55	2.88	0.42	2.72	0.66	2.05	1.89	0.31	0.50	4.07
GP5, M	29.1	43.1	12.8	2.06	7.17	1.42	0.38	2.10	0.32	2.18	0.56	1.75	1.51	0.24	0.67	4.27
GP6, M	38.7	94.3	30.8	4.52	13.8	2.31	0.59	3.17	0.45	2.95	0.73	2.23	1.97	0.32	0.65	3.26
GP7, M	18.4	150	40.6	5.50	15.4	3.17	0.61	2.89	0.38	2.24	0.50	1.33	0.89	0.14	0.65	3.62
GP8, M	7.0	42.8	13.3	2.05	7.20	1.22	0.27	1.19	0.15	0.82	0.18	0.51	0.42	0.069	0.71	4.36
GP9, M	20.8	117	39.4	6.14	21.0	3.55	0.85	4.00	0.47	2.32	0.42	0.96	0.69	0.10	0.69	3.74
GP10, 10	12.6	70.7	19.6	2.80	8.36	1.41	0.34	1.62	0.23	1.39	0.31	0.92	0.85	0.14	0.65	3.78
Feet																
GP5, F	9.20	41.2	11.5	1.46	4.30	0.83	0.21	1.16	0.15	0.96	0.22	0.64	0.56	0.10	0.73	4.14
GP7, F	4.76	47.7	12.4	1.61	4.17	0.70	0.14	0.71	0.085	0.52	0.12	0.35	0.33	0.065	0.63	3.39
Haslets																
GP2, H	21.6	255	64.7	9.7	27.1	4.72	1.07	4.83	0.63	3.44	0.66	1.77	1.87	0.31	0.59	3.52
GP7, H	113	547	217	29.0	95.3	20.6	4.95	20.6	3.12	17.7	3.45	9.48	9.45	1.34	0.77	3.42

Table S-3 REE and Y abundances (in ng/g) in *Bathylomodius aduloides* from Site F (S: shell; G: gill; M: mantle).

	Y	La	Ce	Pr	Nd	Sm	Eu	Gd	Tb	Dy	Ho	Er	Yb	Lu	Ce/Ce*	La/La*
Shells																
BA1, S	61.8	48.7	44.7	7.67	33.0	6.74	1.74	8.49	1.07	5.97	1.22	3.21	2.61	0.41	0.78	1.98
BA2, S	60.9	64.0	51.7	8.24	33.7	5.94	1.49	7.66	0.92	4.80	0.96	2.26	1.38	0.21	0.80	2.19
BA3, S	56.1	57.1	43.4	7.34	30.1	5.29	1.30	6.67	0.84	4.60	0.94	2.31	1.63	0.26	0.76	2.20
Gill																
BA2, G	242	71.1	85.6	16.3	90.2	34.6	7.82	36.6	4.86	26.5	5.27	13.8	13.5	2.42	0.91	2.26
Mantle																
BA2, M	151	88.6	139	22.4	117	34.5	9.29	42.4	5.48	28.3	5.20	11.6	6.56	0.91	1.02	1.83

Table S-4 REE and Y abundances (in ng/g) in *Gigantidas Haimaensis* from Haima (S: shell; F: foot; G: gill; M: mantle).

	Y	La	Ce	Pr	Nd	Sm	Eu	Gd	Tb	Dy	Ho	Er	Yb	Lu	Ce/Ce*	La/La*
Shells																
GH1, S	25.9	77.4	51.5	4.97	15.3	2.32	0.52	3.03	0.35	2.10	0.47	1.31	1.20	0.19	1.00	2.50
GH2, S	25.2	41.2	26.8	3.12	10.8	2.11	0.50	2.76	0.35	2.08	0.46	1.30	1.19	0.19	0.93	2.65
GH3, S	43.3	51.9	24.7	2.77	9.75	2.20	0.62	3.65	0.52	3.42	0.83	2.52	2.52	0.43	0.98	3.92
GH4, S	28.1	27.9	16.4	1.97	6.77	1.41	0.37	2.25	0.31	2.05	0.49	1.47	1.38	0.23	0.90	2.84
GH5, S	27.1	61.3	29.0	3.36	11.1	1.93	0.48	2.82	0.34	2.12	0.49	1.39	1.25	0.20	0.89	3.35
Mantles																
GH1, M	63.0	281	247	25.2	83.9	15.1	3.02	15.3	1.73	9.40	1.85	4.81	3.73	0.52	1.02	2.08
GH2, M	9.40	63.8	27.6	2.83	7.19	1.93	0.30	1.62	0.18	0.94	0.17	0.41	0.37	0.059	0.78	2.45
GH3, M	57.9	265	182	14.0	36.6	6.54	1.53	8.85	1.03	6.07	1.31	3.48	2.48	0.33	1.07	2.19
GH4, M	27.4	115	73.3	6.80	20.3	4.01	0.84	4.27	0.53	2.92	0.58	1.47	1.19	0.18	1.01	2.53
GH5, M	33.0	141	95.7	7.84	21.3	3.60	0.89	4.83	0.65	4.11	0.98	2.86	2.27	0.34	1.03	2.22
Feet																
GH1, F	31.8	219	161	15.7	48.2	7.88	1.58	8.62	0.89	4.84	0.97	2.54	2.05	0.30	0.98	2.21
GH2, F	5.32	39.4	17.7	1.57	4.06	0.81	0.15	0.86	0.10	0.61	0.13	0.36	0.39	0.068	0.91	2.81
GH3, F	15.8	114	73.4	5.36	12.8	1.86	0.42	2.86	0.27	1.71	0.37	1.04	0.95	0.15	1.02	2.04
GH4, F	10.2	51.7	33.1	2.78	7.39	1.16	0.27	1.49	0.18	1.12	0.25	0.66	0.61	0.098	0.99	2.22
GH5, F	11.2	67.4	42.4	3.26	7.84	1.16	0.25	1.41	0.18	1.23	0.29	0.89	0.93	0.16	0.98	2.01
Gills																
GH2, G	23.6	1827	446	53.7	77.0	6.24	1.17	7.39	0.57	3.03	0.59	1.52	1.39	0.25	0.37	1.18
GH3, G	47.5	840	374	34.4	69.4	9.76	1.98	14.2	1.15	5.91	1.09	2.63	2.30	0.36	0.69	1.67
GH4, G	39.3	862	263	31.4	58.3	9.13	1.59	8.68	0.91	4.51	0.80	1.85	1.60	0.26	0.49	1.60
GH5, G	37.9	773	285	23.4	44.2	6.12	1.25	7.18	0.79	4.48	0.95	2.55	2.36	0.40	0.72	1.99

Table S-5 REE and Y abundances (in ng/g) in *Calyptogena marissinica* from Haima (S: shell; G: gill; M: mantle).

	Y	La	Ce	Pr	Nd	Sm	Eu	Gd	Tb	Dy	Ho	Er	Yb	Lu	Ce/Ce*	La/La*
Shells																
CM1, S	3.55	5.43	10.1	1.23	4.67	0.95	0.19	0.89	0.10	0.59	0.11	0.28	0.23	0.031	0.975	1.073
CM2, S	20.5	27.9	57.4	6.62	25.8	5.28	1.10	5.07	0.63	3.37	0.64	1.65	1.38	0.19	1.06	1.08
Mantles																
CM1, M	849	743	1087	154	627	139	32.2	154	20.5	111	21.5	54.2	40.5	5.80	0.90	1.34
CM2, M	1352	1215	1534	231	941	203	46.6	220	27.8	128	20.1	43.3	29.6	3.91	0.84	1.47
Gills																
CM1, G	211	154	86.7	22.1	93.5	20.2	5.18	27.6	3.41	18.5	3.75	9.23	6.25	0.93	0.52	2.10
CM2, G	888	706	463	102	422	85.3	20.9	111	13.9	76.5	15.8	39.5	27.9	4.44	0.59	2.00

Table S-6 REE abundances in *Calyptogena* shells (in ng/g) from Nankai Trough (n.a: not analysed).

	Y	La	Ce	Pr	Nd	Sm	Eu	Gd	Tb	Dy	Ho	Er	Yb	Lu	Ce/Ce*	La/La*
KN1-A	n.a.	58.7	68.7	8.84	30.02	5.45	1.35	6.61	0.99	5.36	1.01	2.47	1.56	0.21	0.83	1.29
KN1-(2)	n.a.	1474	2487	224	814	128	30.66	139	19.13	102	18.26	40.76	22.94	2.97	1.26	1.46
KN2	n.a.	51.9	33.0	5.29	19.93	3.65	0.94	4.30	0.54	2.70	0.55	1.35	0.76	0.12	0.73	2.34
KN7	n.a.	250	442	41.9	140	22.60	5.13	25.10	3.60	19.65	3.80	9.04	5.78	0.78	1.10	1.13
KN14-(2)	n.a.	51.5	75.5	8.11	27.87	5.27	1.02	5.90	0.97	5.75	1.22	3.28	2.49	0.33	1.00	1.27

Table S-7 REE and Y concentrations (in ng/g) in *Mytilus edulis* (S: shell; ST: soft tissue) from Brittany (Ouessant) and Normandy (Chausey and Gouville/Mer), France.

	Y	La	Ce	Pr	Nd	Sm	Eu	Gd	Tb	Dy	Ho	Er	Yb	Lu	Ce/Ce*	La/La*
Ouessant																
Ou1, S	7.54	5.69	4.89	0.80	3.62	0.84	0.20	1.19	0.13	0.66	0.12	0.25	0.10	0.012	0.86	2.43
Ou2, S	5.97	7.72	6.00	1.03	3.93	0.79	0.17	1.06	0.10	0.50	0.092	0.20	0.11	0.015	0.70	1.84
Ou3, S	6.35	6.76	5.81	0.90	3.56	0.73	0.17	1.02	0.11	0.54	0.096	0.21	0.087	0.014	0.80	2.00
Ou4, S	7.11	6.93	5.62	0.88	3.69	0.76	0.17	1.07	0.11	0.57	0.11	0.25	0.13	0.017	0.84	2.33
Ou1, ST	23.7	51.6	59.0	6.79	25.6	4.67	0.99	4.68	0.57	3.13	0.61	1.59	1.38	0.23	1.02	1.82
Ou2, ST	18.3	46.6	46.6	5.34	20.3	4.10	0.82	3.91	0.49	2.54	0.47	1.17	0.98	0.15	1.04	2.13
Ou4, ST	39.2	66.0	64.4	8.14	33.9	7.10	1.57	7.84	0.98	5.20	1.02	2.59	2.15	0.34	1.03	2.38
Chausey																
Ch1, S	12.6	9.89	16.1	1.99	8.28	1.69	0.39	2.06	0.23	1.16	0.20	0.46	0.33	0.044	1.05	1.45
Ch2, S	10.4	8.47	11.9	1.56	6.53	1.28	0.29	1.57	0.18	0.97	0.19	0.48	0.34	0.048	1.00	1.60
Ch3, S	10.7	8.48	11.4	1.49	6.34	1.20	0.29	1.55	0.18	0.99	0.20	0.49	0.30	0.040	1.02	1.74
Gouville/Mer																
Go1, S	9.12	8.31	12.3	1.60	6.55	1.36	0.31	1.57	0.19	1.03	0.20	0.48	0.33	0.044	0.99	1.48
Go2, S	13.3	9.48	13.3	1.78	7.57	1.59	0.39	2.08	0.24	1.23	0.23	0.52	0.32	0.044	0.99	1.62
Go3, S	8.93	8.82	10.9	1.37	5.74	1.12	0.26	1.44	0.17	0.90	0.18	0.42	0.25	0.035	1.03	1.89

Table S-8 REE and Y abundances (µg/g) in terrigeneous sediments from Haima, Site F, and results for USGS basalt BCR2.

	Y	La	Ce	Pr	Nd	Sm	Eu	Gd	Tb	Dy	Ho	Er	Yb	Lu	Ce/Ce*	La/La*
Site F, sediments																
LN1	20.93	33.67	69.66	7.75	28.70	5.35	1.09	4.59	0.64	3.63	0.72	1.99	1.91	0.276	1.04	1.00
LN10	22.10	36.89	74.77	8.33	31.26	5.86	1.17	4.95	0.69	3.86	0.76	2.12	2.01	0.291	1.05	1.05
Haima, sediments																
mussel zone	23.21	32.52	67.09	7.53	28.16	5.40	1.09	4.79	0.69	3.95	0.78	2.21	2.10	0.302	1.04	1.02
clam zone	21.24	28.29	56.99	6.47	24.10	4.61	0.94	4.21	0.60	3.43	0.70	1.95	1.82	0.263	1.03	1.02
BCR2 (three distinct dissolutions)																
#1	38.08	25.80	54.53	6.91	29.07	6.60	1.93	6.83	1.06	6.43	1.32	3.65	3.36	0.490	1.04	1.11
#2	37.99	25.86	54.54	6.96	29.19	6.65	1.94	6.87	1.06	6.42	1.33	3.66	3.38	0.492	1.03	1.10
#3	37.92	24.84	52.70	6.82	28.75	6.58	1.90	6.72	1.05	6.39	1.31	3.64	3.40	0.486	1.02	1.09
average (n=3)	**38.00**	**25.50**	**53.92**	**6.90**	**29.00**	**6.61**	**1.92**	**6.81**	**1.06**	**6.41**	**1.32**	**3.65**	**3.38**	**0.489**	**1.03**	**1.10**
RSD (%)	*0.21*	*2.25*	*1.97*	*0.99*	*0.78*	*0.57*	*1.05*	*1.14*	*0.64*	*0.30*	*0.48*	*0.32*	*0.45*	*0.66*	*1.00*	*1.10*
Jochum *et al.* (2016)	36.07	25.08	53.12	6.83	28.26	6.55	1.99	6.81	1.08	6.42	1.31	3.67	3.39	0.50	1.01	1.06

Table S-9 REE and Y abundances REE+Y abundances (in ng/g) in Cal-S standard obtained during the course of this study.

	Y	La	Ce	Pr	Nd	Sm	Eu	Gd	Tb	Dy	Ho	Er	Yb	Lu	Ce/Ce*	La/La*
average, n=41	**2177**	**806**	**313**	**89.2**	**363**	**63.7**	**15.9**	**92.3**	**13.9**	**99.6**	**26.3**	**82.0**	**67.1**	**10.3**	**0.45**	**2.52**
RSD (%)	*3.58*	*1.33*	*2.72*	*1.70*	*1.70*	*1.68*	*1.33*	*1.41*	*1.23*	*1.29*	*1.12*	*1.11*	*1.23*	*1.22*	*1.23*	*0.80*
Le Goff *et al.* (2019)	2065	793	302	87.1	359	62.4	15.5	91.6	13.7	98.3	26.0	81.0	66.3	10.16	0.45	2.62
Potts *et al.* (2000)	1944	787	333	90	357	64	16	93	14	100	26	81	68	11	0.46	2.63

Supplementary Information References

Barrat, J.A., Keller, F., Amossé, J., Taylor, R., Nesbitt, R., Hirata, T. (1996) Determination of rare earth elements in sixteen silicate reference samples by ICP-MS after Tm addition and ion exchange separation. *Geostandards Newsletter* 20, 133-139.

Barrat, J.A., Bayon, G., Wang, X., Le Goff, S., Rouget, M.L., Gueguen, B., Ben Salem, D. (2020) A new chemical separation procedure for the determination of rare earth elements and yttrium abundances in carbonates by ICP-MS. Talanta, doi.org/10.1016/j.talanta.2020.121244.

Barrat, J.-A., Dauphas, N., Gillet, P., Bollinger, C., Etoubleau, J., Bischoff, A., Yamaguchi, A. (2016) Evidence from Tm anomalies for non-CI refractory lithophile element proportions in terrestrial planets and achondrites. *Geochimica et Cosmochimica Acta* 176, 1-17.

Jochum, K.P., Weis, U., Schwager, B., Stoll, B., Wilson, S.A., Haug, G.A., Andreae, M.O., Enzweiler, J. (2016) Reference values following ISO guidelines for frequently requested rock reference materials. *Geostandards and Geoanalytical Research* 40, 3, 333-350.

Le Goff, S., Barrat, J.A., Chauvaud, L., Paulet, Y.M., Gueguen, B., Ben Salem, D. (2019) Compound-specific recording of gadolinium pollution in coastal waters by great scallops. *Scientific Reports* 9, 8015.

Potts, P.J., Thompson, M., Kane, J.S., Webb, P.C., Carignan, J. (2000) GeoPT6. An international proficiency test. for analytical geochemistry laboratories - report on round 6 (OU3: Nanhoron microgranite) and 6A (CAL-S: CRPG limestone). *Geostandards Newsletter* 24, E1–E37.